

BCSJ Award Article

Guest-Induced Supramolecular Isomerism and Chirality of Brucine Inclusion Crystals with Aliphatic Alcohols: A Hierarchical Interpretation

Tsuyoshi Watabe, Kenji Kobayashi, Ichiro Hisaki,* Norimitsu Tohnai, and Mikiji Miyata*

Department of Material and Life Science, Graduate School of Engineering, Osaka University, 2-1 Yamadaoka, Suita, Osaka 565-0871

Received September 6, 2006; E-mail: miyata@mls.eng.osaka-u.ac.jp

Cocrystallization of brucine with a series of aliphatic alcohols was systematically investigated to understand molecular recognition through supramolecular isomerism and chirality. Guest-induced supramolecular isomers of brucine were obtained by cocrystallization and were categorized into three structural types based on the common 2_1 helical tape-like assemblies. These supramolecular isomers were elucidated from the molecular structures on the basis of qualitative hierarchical structural analysis through supramolecular chirality. Moreover, it was found that the supramolecular isomerization occurred depending on the size of the guest molecules. This dependence was clearly evaluated on the relationship between the volume of the guest molecules and the packing coefficient of the void spaces in the host cavities.

Crystalline host compounds have attracted much attention in the field of crystal engineering and supramolecular chemistry due to practical and fundamental applications in catalysis, magnetism, electro and non-linear optics, chemical separation, gas-storage, and drug delivery.[1–5] Interestingly, their host frameworks are isomerized in response to host–guest hydrogen-bonding interactions and shape/size of the guests.[6–9] Guest-induced supramolecular isomerism of host frameworks with nanosize pores has been seen as a problem from a design perspective of the inclusion properties. However, it is also possible to view the guest-induced supramolecular isomerism as an opportunity to gain better fundamental understanding of cocrystallization and molecular recognition. To understand the guest-induced supramolecular isomerism, we have so far prepared over three hundreds inclusion crystals of steroidal bile acids, and elucidated their supramolecular isomeric structures starting from single molecular structures.[10–16] On the basis of a series of the studies, we have proposed that the supramolecular isomerism in their inclusion crystals can be interpreted by the hierarchical structural analysis through supramolecular chirality.[12–18] The structural analysis is performed in the following four phases (Scheme 1): (i) fixing a conformation of a host molecule with three-directional chirality,[16] i.e., head and tail (or leg), right and left, and belly and back, (ii) forming a bimolecular aggregate and stacking of the bimolecular aggregate to form a motif, such as columnar assembly with the three-directional chirality, (iii) stacking the columns in a parallel or anti-parallel fashion to produce a bundle of the columns, (iv) accommodating guest molecules in the cavities of the bundles to yield host–guest complexes characterized by molecular recognition. It is noteworthy that the chirality of a single molecule dominates the supramolecular chirality of the columns, bundles, and complexes in the corresponding steps. We believe that the concept of three-directional chirality for structurally analyzed supramolecular architectures, such as crystal structures, must serve as a widely useful approach to treat complicated self-assembled systems with chirality.

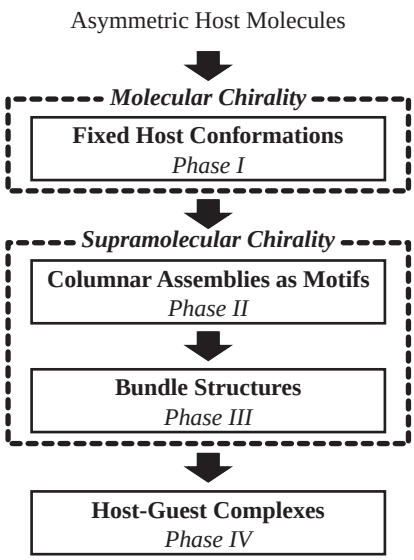

Scheme 1. Hierarchical structural analysis of supramolecular isomerism of host–guest complexes.

The hierarchical structural analysis has been focused on

Published on the web March 13, 2007; doi:10.1246/bcsj.80.464

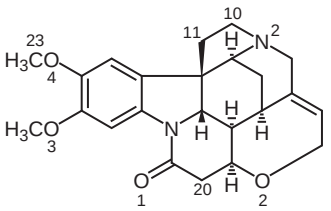

Scheme 2. Molecular structure of brucine with selected atomic numbers.

hydrogen-bond interactions, because the steroidal bile acids form inclusion crystals via multiple and cooperative hydrogen bonds.[12–16] However, it is not clear whether the analysis is a useful approach for the structural elucidation of the supramolecular isomers constructed with intermolecular interactions weaker than hydrogen bonds. Our aim in this study has been to extend the applicability of the proposed structural analysis to a chiral compound without hydrogen-bonding donor groups.

Brucine (Scheme 2), which is a natural host compound with six asymmetric carbon atoms and no hydrogen-bonding donor group, has been historically investigated as a separator of racemic mixtures by cocrystallization generally with guest molecules containing acidic functional groups.[19–29] According to the studies performed by Gould and Walkinshaw,[19,24] brucine forms a characteristic corrugated monolayer sheet as a motif common to its many inclusion crystals, in spite of appearance of supramolecular isomeric host frameworks. The motifs are stabilized by weak hydrogen bonds, such as CH/O and CH/π interactions.[29] However, to our knowledge, the supramolecular isomerism of the host frameworks of brucine has been discussed ambiguously. Because of these aspects, brucine is a good starting point for extending the applicability of the hierarchical structural analysis to better understand supramolecular isomerism. Recently, we obtained the supramolecular isomeric host frameworks in brucine inclusion crystals with a series of aliphatic alcohols.[17] In this paper, we describe the structural elucidation of these supramolecular isomers starting from the molecules and demonstrate that the qualitative hierarchical structural analysis through supramolecular chirality is a useful approach for understanding supramolecular isomerism and cocrystallization.

Results and Discussion

Inclusion Crystal Structures of Brucine with Aliphatic Alcohols. Results of crystallization studies of brucine with a series of aliphatic alcohols including racemic mixtures are shown in Table 1. The recrystallization of brucine from the aliphatic alcohols afforded the known guest-free,[30] and eleven new inclusion crystals. These inclusion crystal structures were determined by X-ray crystallography. Their crystallographic parameters are summarized in Table 2. The inclusion crystals had a 1:2 or 1:1 host/guest molar ratio and belonged to the space group $P2_12_12_1$. The resultant crystal structures are depicted in Figs. 1 and 2. The primary interactions in the brucine inclusion crystals with aliphatic alcohols were hydrogen bonds between the alcohol functionality of the guests and the hydrogen-bonding acceptor groups of brucine. The crystal with **1** had $O_{guest(B)}$–H···$O_{guest(A)}$–H···N2 (N2: tertiary amino) hydrogen bonds with lengths of 2.790 and 2.780 Å, respectively.

Table 1. Aliphatic Alcohols Used for Cocrystallization with Brucine, and Host/Guest Molar Ratio of Resultant Crystals

Guest		Host/guest molar ratio[a)]
1	Methanol	1:2
2	Ethanol	GF[b)]
3	1-Propanol	1:1
4	2-Propanol	GF
5	1-Butanol	NC[c)]
6	2-Butanol	GF
7	2-Methyl-1-propanol	1:1
8	2-Methyl-2-propanol	1:1
9	1-Pentanol	GF
10	2-Pentanol	GF
11	3-Pentanol	GF
12	2-Methyl-1-butanol	1:1
13	2-Methyl-2-butanol	1:1
14	3-Methyl-1-butanol	1:1
15	3-Methyl-2-butanol	1:1
16	1-Hexanol	GF
17	2-Hexanol	GF
18	3-Hexanol	NC
19	2-Methyl-1-pentanol	NC
20	2-Methyl-2-pentanol	GF
21	2-Methyl-3-pentanol	GF
22	3-Methyl-1-pentanol	GF
23	3-Methyl-2-pentanol	NC
24	3-Methyl-3-pentanol	1:1
25	4-Methyl-1-pentanol	GF
26	4-Methyl-2-pentanol	GF
27	2,3-Dimethyl-2-butanol	NC
28	3,3-Dimethyl-1-butanol	NC
29	3,3-Dimethyl-2-butanol	1:1
30	2-Ethyl-1-butanol	GF
31	1-Heptanol	GF
32	2-Heptanol	NC
33	3-Heptanol	GF
34	4-Heptanol	GF
35	2,4-Dimethyl-3-pentanol	1:1

a) Molar ratios of guest-disordered crystals were determined by TG, see Supporting Information. b) GF denotes guest-free crystals. c) NC denotes no crystallization.

The crystals with **7**, **29**, and **35** have O_{guest}–H···N2 (N2: tertiary amino) hydrogen bonds with lengths of 2.783, 2.876, and 2.818 Å, respectively. In addition, IR spectra of the crystals with **3**, **12**, and **14** (Supporting Information) indicated that the crystals also had O_{guest}–H···N2 (N2: tertiary amino) hydrogen bonds, even though the assignments of the guest molecules could not be determined by X-ray crystallography due to disorder. While, the crystals with **8**, **13**, and **24** had O_{guest}–H···O1 (O1: carbonyl) hydrogen bonds with lengths of 2.861, 3.064, and 2.868 Å, respectively. Furthermore, IR spectrum of the crystal of **15** (Supporting Information) showed that a O_{guest}–H···O1 (O1: carbonyl) hydrogen bond was present, even though the assignment of the guest molecule could not be performed by X-ray crystallography due to disorder.

The inclusion crystal of **1** has a similar host framework to those of brucine dihydrates of **2** and **4**.[30,31] However, the inclusion crystals with **3**, **7**, **8**, **12**, **13**, **14**, **15**, **24**, **29**, and **35** have a

Table 2. Crystallographic Parameters of Brucine Inclusion Crystals with Aliphatic Alcohols

	Brucine·**1**	Brucine·**3**	Brucine·**7**	Brucine·**8**	Brucine·**12**	Brucine·**13**	Brucine·**14**	Brucine·**15**	Brucine·**24**	Brucine·**29**	Brucine·**35**
Formula	$C_{23}H_{26}N_2O_4\cdot 2CH_4O$	$C_{23}H_{26}N_2O_4\cdot C_3H_8O$	$C_{23}H_{26}N_2O_4\cdot C_4H_{10}O$	$C_{23}H_{26}N_2O_4\cdot C_4H_{10}O$	$C_{23}H_{26}N_2O_4\cdot C_5H_{12}O$	$C_{23}H_{26}N_2O_4\cdot C_5H_{12}O$	$C_{23}H_{26}N_2O_4\cdot C_5H_{12}O$	$C_{23}H_{26}N_2O_4\cdot C_5H_{12}O$	$C_{23}H_{26}N_2O_4\cdot C_6H_{14}O$	$C_{23}H_{26}N_2O_4\cdot C_6H_{14}O$	$C_{23}H_{26}N_2O_4\cdot C_7H_{16}O$
T/K	198	296	198	213	93	213	203	198	296	296	198
Crystal system	orthorhombic	orthorhombic	orthorhombic	orthorhombic	orthorhombic	orthorhombic	orthorhombic	orthorhombic	orthorhombic	orthorhombic	orthorhombic
Space group	$P2_12_12_1$ (No. 19)	$P2_12_12_1$ (No. 19)	$P2_12_12_1$ (No. 19)	$P2_12_12_1$ (No. 19)	$P2_12_12_1$ (No. 19)	$P2_12_12_1$ (No. 19)	$P2_12_12_1$ (No. 19)	$P2_12_12_1$ (No. 19)	$P2_12_12_1$ (No. 19)	$P2_12_12_1$ (No. 19)	$P2_12_12_1$ (No. 19)
Z	4	4	4	4	4	4	4	4	4	4	4
a/Å	12.0807(7)	13.649(1)	13.687(4)	12.3966(3)	14.016(4)	14.04(1)	12.403(3)	14.0830(8)	12.89(1)	13.8095(9)	13.662(1)
b/Å	25.071(1)	14.196(1)	14.202(4)	13.5716(3)	14.016(3)	14.28(1)	13.545(4)	14.4117(8)	14.148(10)	15.077(1)	15.9283(9)
c/Å	7.6303(4)	12.374(1)	12.355(3)	14.3334(3)	12.443(2)	12.550(7)	14.448(4)	12.3314(5)	14.497(9)	12.4165(6)	12.3820(7)
α/°	90	90	90	90	90	90	90	90	90	90	90
β/°	90	90	90	90	90	90	90	90	90	90	90
γ/°	90	90	90	90	90	90	90	90	90	90	90
V/Å^3	2311.1(2)	2397.6(4)	2401(1)	2411.5(1)	2444(1)	2515(3)	2427(1)	2502.8(2)	2644(3)	2585.1(3)	2694.6(3)
ρ_{calcd}/g cm^{-3}	1.318	1.259	1.296	1.291	1.311	1.274	1.321	1.281	1.247	1.276	1.259
Reflections collected	13854	8128	11909	23302	10378	26160	14143	10078	10517	8596	11281
Independent reflections/R_{int}	2289/0.046	2433/0.024	2362/0.125	2492/0.048	2389/0.050	2543/0.033	2452/0.104	2524/0.072	2584/0.047	2638/0.044	2582/0.041
Goodness-of-fit on F^2	1.73	1.98	1.07	1.65	1.42	1.06	1.83	1.02	2.44	1.38	1.40
R_1/wR^2	0.050/0.133	0.063/0.191	0.086/0.228	0.068/0.169	0.075/0.170	0.076/0.197	0.121/0.276	0.080/0.203	0.086/0.223	0.062/0.161	0.035/0.094

similar host framework to those of brucine with bicyclo[2.2.1]-hept-5-ene-2-cyanohydrins,[32] and pantolactone.[33] All the resultant crystals could be categorized into three structural types of supramolecular isomers composed of common 2_1 helical tape-like assemblies stabilized by weak multiple hydrogen bonds, such as CH/O and CH/π interactions:[29] C10–H···O3, C11–H···O4 (O3 and O4: methoxy), C23–H···O2 (O2: ether), and C20–H···π (arene) hydrogen bonds as shown in Fig. 3.

To clarify the factors of supramolecular isomerization, we carried out a comparative structural study of the resultant crystals. From the comparative study, it was believed that their crystals have hierarchical structures in common as described below (Fig. 4).

In this method, the molecule is first regarded as a primary structure for making the subsequent molecular architecture (Fig. 4a). Second, the molecules are presumed to associate together to produce a bimolecular assembly followed by expansion into a helical tape-like assembly as a secondary structure (Fig. 4b). Third, the helical tapes are thought to combine producing a bundle of the tapes as a tertiary structure (Fig. 4c). Finally, the bundles leave the cavities for accommodating guest components to yield a host–guest complex as a quaternary structure (Fig. 4d). Although the order of these phases in the hierarchical structure does not necessarily correspond to the real process of crystal formation, this concept showed a powerful method for understanding the cocrystallization.

To clarify the ambiguous cocrystallization process, we next discuss supramolecular isomerism starting from the chirality of single molecules, and then helical tape-like assemblies, bundles, and complexes will be discussed in this order.

Phase I: Primary Structures as Molecular Conformations and Chirality of Brucine in Its Inclusion Crystals. In the first phase, we considered the fixation of molecuar conformation of brucine. As can be expected from the chemical structure, the structure of brucine dose not vary much including rotation of the methoxy substituent groups, which are invariably *anti*-related and lie essentially in the same plane of the benzene ring (Fig. 5).[34] Actually, the same molecular conformation has been observed in all known crystals of brucine,[30] brucine solvates,[30,31,34] brucine complexes,[32,33,35–37] and brucinium salts.[19–29,38–45] Such a conformer of brucine was observed in all the resultant crystals with aliphatic alcohols with no exception. Therefore, it may be assumed that brucine molecule exists in solution as a predominant conformer. Such an assumption leads to the fixation of the molecular conformation during crystallization process and has been adopted in an attempt to predict crystal structures in a more realistic manner.[46–49]

Having fixed the molecular conformation of brucine, we now discuss the expression of three-dimensional asymmetry of the single chiral molecule. Three-dimensional asymmetry means that the asymmetry of the molecules involves multiple asymmetric carbon atoms and is useful for geometrical visualization of the supramolecular chiral aggregates.[12–17] Conventionally, molecular asymmetry has been expressed by using terms such as center, axis, and plane of chirality. However, in the case of the molecules with multiple asymmetric carbon atoms, such terms can be used to describe a part of the molecular structure, but not the entire structure. Therefore, we have

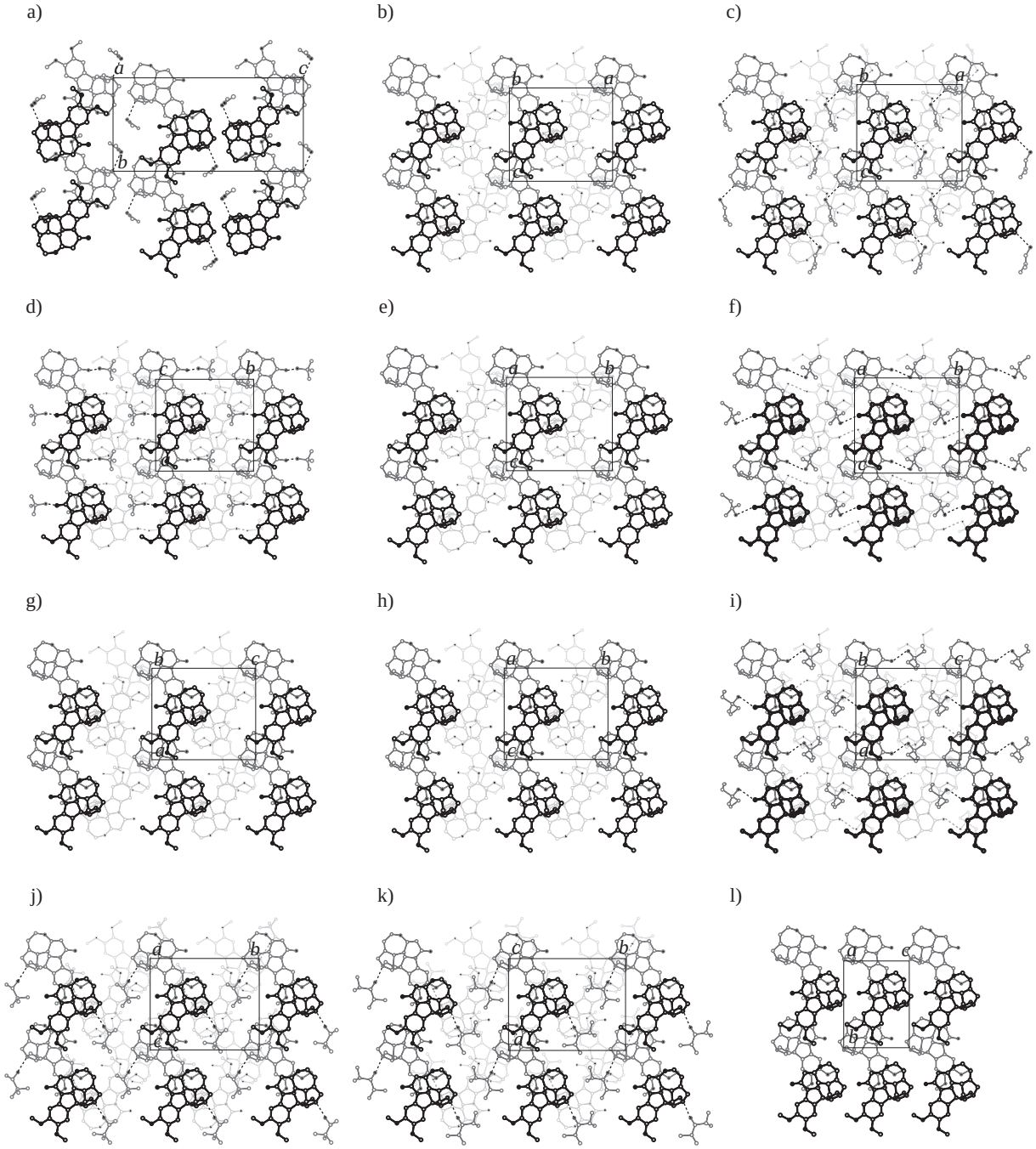

Fig. 1. Side views of the crystal structures of a) brucine•**1**, b) brucine•**3**, c) brucine•**7**, d) brucine•**8**, e) brucine•**12**, f) brucine•**13**, g) brucine•**14**, h) brucine•**15**, i) brucine•**24**, j) brucine•**29**, k) brucine•**35**, and l) brucine guest-free.[32] Hydrogen atoms have been omitted for clarity. Carbon, nitrogen, and oxygen atoms are represented by white, gray, and black spheres, respectively. Dashed lines mean hydrogen bonds between host and guest molecules. In the crystals of brucine with **3**, **12**, **14**, and **15**, the positions of the guest molecules, which can not be determined due to disorder, have been hidden.

proposed a new method for describing molecular asymmetry. In addition, by using this method, we defined the supramolecular chirality of the molecular aggregates in the secondary structures.[12–17] We expressed the three-dimensional asymmetry of brucine molecule on the basis of the new method as mentioned below.

Brucine has an asymmetric facial shape, since it consists of polycyclic and planar skeletons with six asymmetric carbon atoms. As shown in Fig. 5, we noticed that the molecules are similar to vertebrate animals with three distinguishable directions. In order to express the directions of animal bodies in our daily life, we use the words: head and tail (or leg), right and left, and belly and back. In the same way, we proposed that such facial asymmetry of the molecules was termed as three-directional chirality[12–16] and that those words may be used for defining the directions. Figure 5 shows the brucine

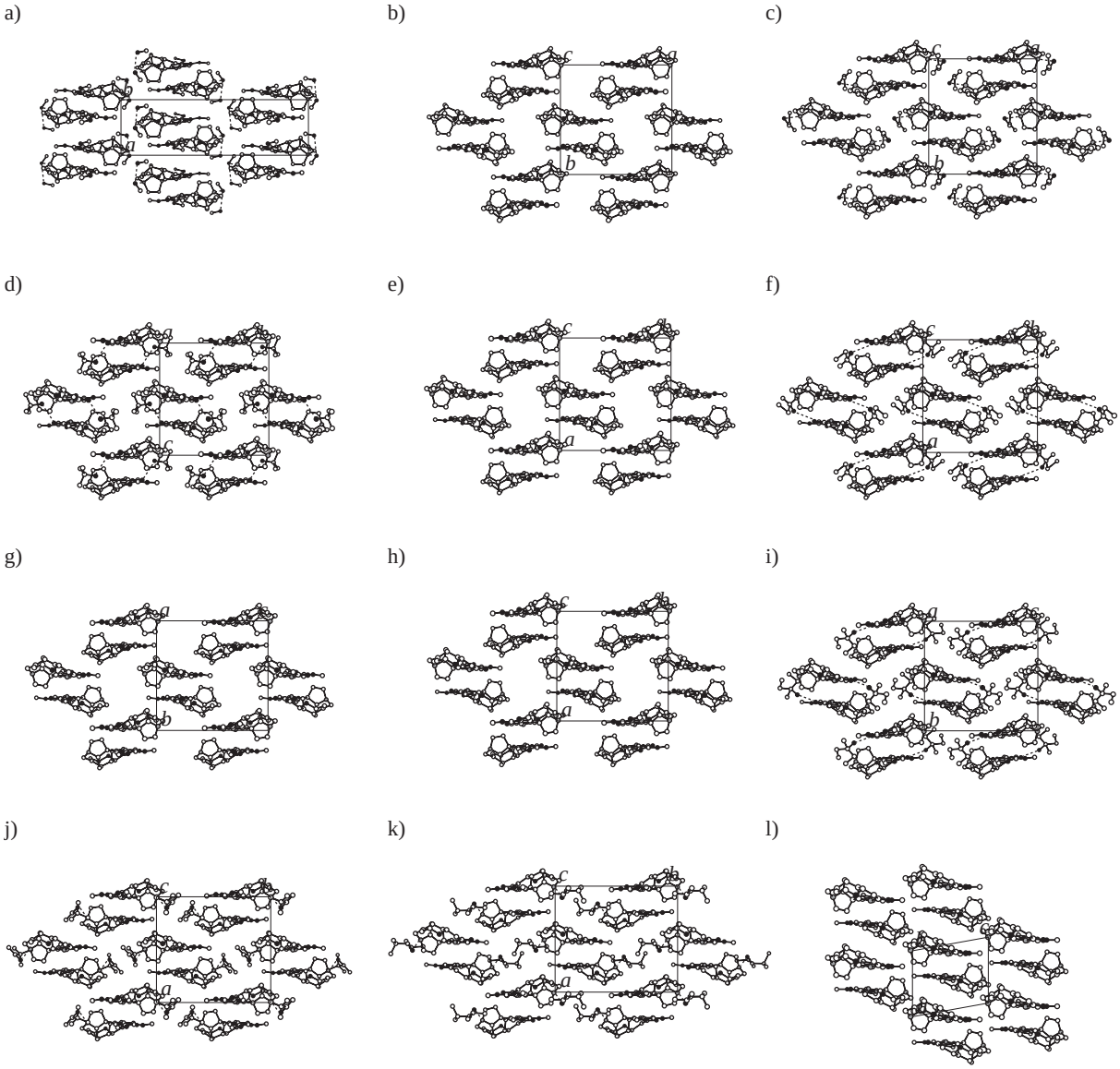

Fig. 2. Top views of the crystal structures of a) brucine•**1**, b) brucine•**3**, c) brucine•**7**, d) brucine•**8**, e) brucine•**12**, f) brucine•**13**, g) brucine•**14**, h) brucine•**15**, i) brucine•**24**, j) brucine•**29**, k) brucine•**35**, and l) brucine guest-free.[32] Hydrogen atoms have been omitted for clarity. Carbon, nitrogen, and oxygen atoms are represented by white, gray, and black spheres, respectively. Dashed lines mean hydrogen bonds between host and guest molecules. In the crystals of brucine•**3**, **12**, **14**, and **15**, the positions of the guest molecules, which can not be determined due to disorder, have been hidden.

molecule displayed with the three-directional chirality: head–leg, right–left, and belly–back axes. The three-directional chirality leads to the definition of the supramolecular chirality of the 2_1 helical tape-like assemblies and host frameworks in the following phases.

Phase II: Secondary Structures as 2_1 Helical Tape-Like Assemblies with Three-Directional Supramolecular Chirality. In the second phase, we focus on asymmetric 2_1 helical tape-like assemblies based on the bimolecular aggregations. The common 2_1 helical tape-like assemblies were observed in all brucine inclusion crystals with aliphatic alcohols as described before. Gould and Walkinshaw have emphasized the tendency to conserve the molecular arrangement of the 2_1 helical tape-like assembly as a motif.[19] On the basis of Kitaigorodskii's report that molecules without symmetry elements predominantly form 2_1 helical assemblies,[50] it is reasonable that brucine molecules assemble into a 2_1 helical tape. However, the helical handedness with a 2_1 axis cannot be determined from the theoretical view point because the screw axis operation includes 180° rotation as well as translation, leading to impossibility to distinguish right- or left-handed rotation.[51] Yet, we believe that the handedness of 2_1 helical assemblies could lead to a better understanding of supramolecular isomerism and chirality and have defined the handedness of 2_1 helical assemblies on the basis of the tilt of the brucine molecule by the following manner.[52]

The handedness was defined on the basis of the relative position of the chiral molecules as schematically shown in Fig. 6a, where assembly *A* has right-handed screw axis and assembly *B* has a left-handed screw axis. Since the structure

of brucine has a convex part at the right side around N2, its neighboring concave part can accommodate two methoxy groups of the other molecule. To accommodate the methoxy groups, the molecule inclines to the right against the screw axis with the belly side as shown in Fig. 6b. As a result, brucine molecules lead to a right-handed helical assembly with the belly-inside. The definition of the three-directional chirality can be used to discriminate among the three axes of the helical assembly: screw-axis, long-axis, and short-axis (Fig. 6c). The helical arrow indicates the leg-to-head direction, which is consistent with the crystallographic 2_1 axis. The three-directional chirality of the asymmetric helical tapes is sufficient enough to categorize the bundle structures as host frameworks at the next phase.

Phase III: Tertiary Structures as Supramolecular Isomeric Bundle Structures of 2_1 Helical Tape-Like Assemblies. The third phase involves the stacking of the asymmetric helical tapes to form bundles of the tapes, which corresponds to the host frameworks. These are four possible combinations of the four tapes with respect to the helical arrow of the tapes (Fig. 7). In Figs. 7a and 7a′, the arrows are parallel to both the long and short axes, and they are anti-parallel to the long axis and parallel to the short axis for Figs. 7b and 7b′, while parallel to the long axis and anti-parallel to the short axis for Figs. 7c and 7c′. In Figs. 7d and 7d′, the arrows are anti-parallel to both long and short axes.

As shown in Figs. 7a and 7a′, the all-parallel stacking leads to the guest-free (GF) crystal with monoclinic symmetry. However, if at least one anti-parallel arrangement is included, the bundle will have orthogonal symmetry. The stacking modes of Figs. 7b, 7b′ and 7c, 7c′ are termed as α-type and β-type structures, respectively. Thus, the resultant crystals of brucine were categorized into three structural types: GF, α-type, and β-type. The host cavities of α-type and β-type structures have different shapes as shown in Fig. 8. The α-type structure, in which the guest molecule **1** is included, has a one-dimensional cavity sandwiched by the corrugated monolayer sheets of the 2_1 helical assemblies (Fig. 8a). On the other hand, the β-type structure, in which the guest molecules **3**, **7**, **8**, **12**, **13**, **14**, **15**, **24**, **29**, and **35**, has a one-dimensional cavity surrounded by four 2_1 helical tape-like assemblies (Fig. 8b). The α-type and β-type structures differ from each other with respect to the channel motifs of the cavities with reference to the screw-axis of the 2_1 helical assemblies. The β-type structures are further classified into sub-types: β_{N2}-type and

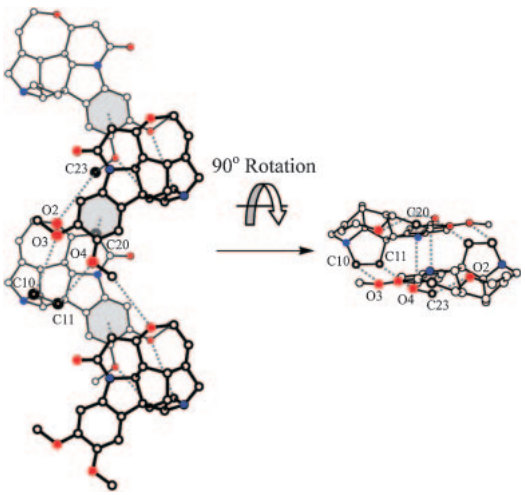

Fig. 3. Side and top views of the helical tape-like assembly of brucine as a motif common to the resultant crystal structures. Dashed lines indicate weak hydrogen bonds, such as CH/O and CH/π interactions. Hydrogen atoms have been omitted for clarity; carbon, nitrogen, and oxygen atoms are represented by white, blue, and red spheres, respectively.

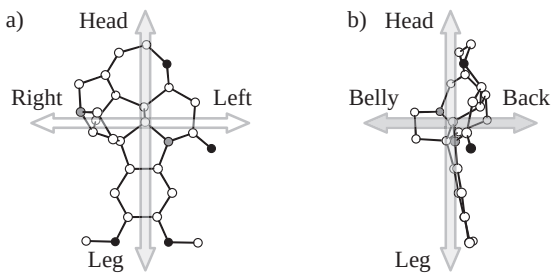

Fig. 5. Molecular conformation of brucine in the crystalline state: a) a front view, and b) a left-side view of the molecule. The molecular chirality of brucine is designated with three axes; head–leg, belly–back, and right–left axes. Hydrogen atoms have been omitted for clarity; carbon, nitrogen, and oxygen atoms are represented by white, gray, and black circles, respectively.

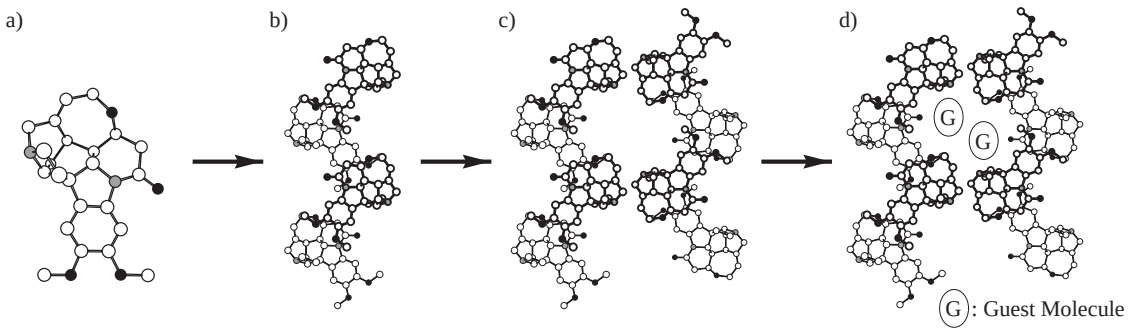

Fig. 4. Hierarchical structural analysis of brucine inclusion crystal structures; a) fixing the molecular conformation, b) combining the bimolecular aggregates to form a helical tape-like assembly, c) stacking the tapes into a bundle, and d) accommodating guest molecules in the cavities of the bundles. Hydrogen atoms have been omitted for clarity; carbon, nitrogen, and oxygen atoms are represented by white, gray, and black spheres, respectively.

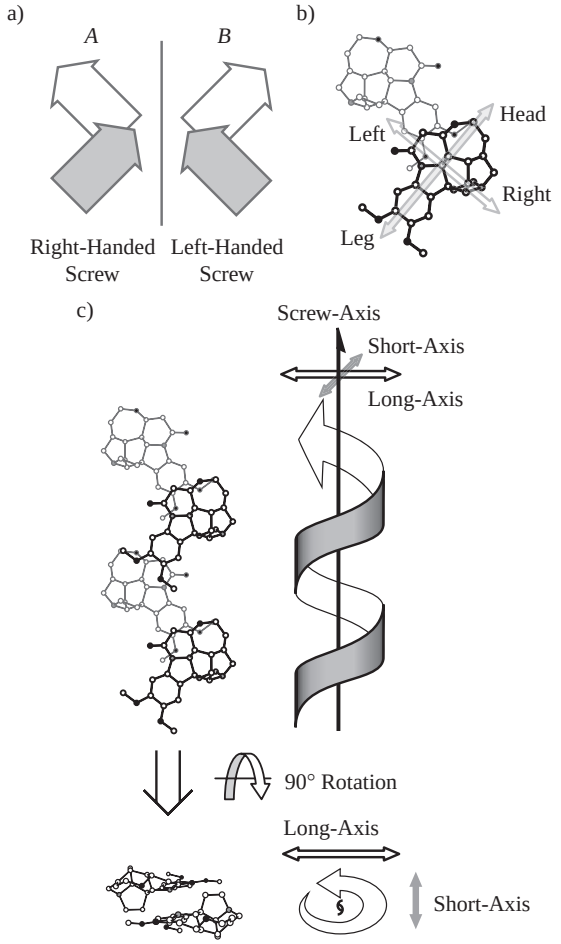

Fig. 6. Supramolecular chirality on the helical tape-like assembly of brucine; a) schematic models of the bimolecular aggregation on the basis of the molecular tilt, where assembly *A* exhibits right-handed screw, while assembly *B* does left-handed screw, b) a side view of the bimolecular aggregate, and c) side and top views of the helical assembly with three distinguishable axes: screw-axis, short-axis, and long-axis. Hydrogen atoms have been omitted for clarity. Carbon, nitrogen, and oxygen atoms are represented by white, gray, and black circles, respectively.

β_{O1}-type structures. The β_{N2}-type and β_{O1}-type structures mean the β-type structure with a O_{guest}–H···N2 (N2: tertiary amino) hydrogen bond, and with a O_{guest}–H···O1 (O1: carbonyl) hydrogen bond, respectively. The relationship between the supramolecular isomeric host frameworks and the guest molecules is summarized in Scheme 3 and will be discussed in the next phase.

Phase IV: Quaternary Structures as Accommodation of Guest Molecules in the Host Cavities. In the final phase, we considered the accommodation of the guest molecules in the cavities of the bundles to yield host–guest complexes. The systematic crystallographic study of brucine inclusion crystals with aliphatic alcohols showed that the host/guest ratios and structural types are dependent mainly on the number of carbons in the guest molecules: one small guest (C1) forms an inclusion crystal with 1:2 host/guest ratio and α-type structure, while ten larger guests (C3–C7) with 1:1 host/guest ratio

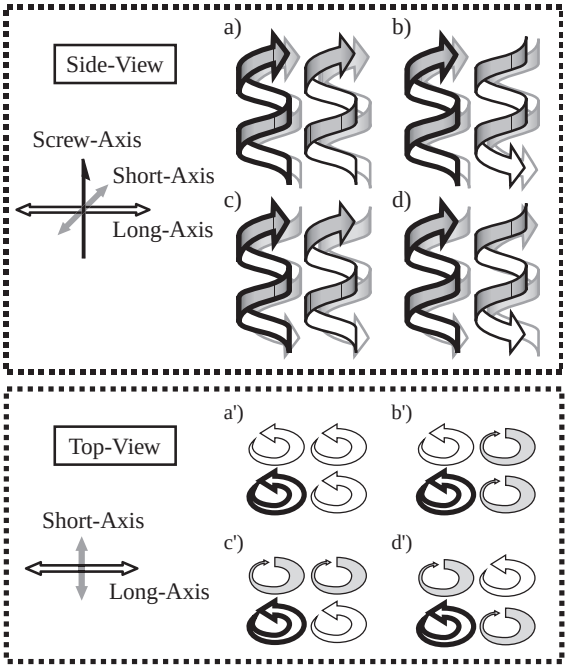

Fig. 7. Bundle structures based on geometrical combination of asymmetric helical tapes: a) and a′) parallel stacking in both long and short axes, b) and b′) anti-parallel stacking in the long axis and parallel in the short axis, c) and c′) parallel stacking in the long axis and anti-parallel stacking in the short axis, and d) and d′) anti-parallel stacking in both long and short axes.

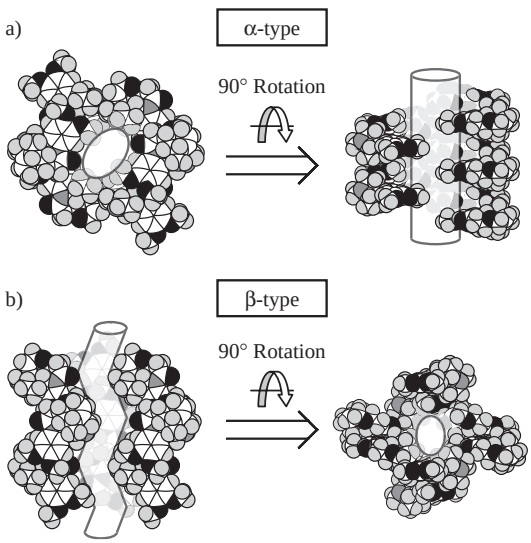

Fig. 8. Views of the one-dimensional cavities in a) α-type structure, and b) β-type structure. The cavities are schematically shown as columns. The host frameworks have been represented by van der Waals space-filling models.

and β-type structure, where C*n* denotes the number of the carbon atoms. In other words, supramolecular isomerism of the host frameworks can be understood in terms of guest size. Since the supramolecular isomerism of the host frameworks is closely related to how well the guest molecules and the host cavity fit together,[53,54] the volumes of the guest molecules and

the host cavities were calculated, as summarized in Table 3.

The packing coefficient of the host cavities (PC_{cavity}), which is the parameter used to estimate the steric fit between the guest molecule and the host cavity,[53] can be determined from their volumes. As listed in Table 3, the PC_{cavity} values of brucine inclusion crystals with aliphatic alcohols were in the range 56–79%, which are larger than those of the encapsulated host compounds in solution (46–64%),[55] and intermediate between those in the liquid state (44–56%)[55] and in the crystalline state (66–77%).[50,56,57] Inclusion crystals with PC_{cavity} values outside of this range would have difficulty forming because of the improper fit between the guest molecule and the host cavity.

Figure 9 shows the relationship between the guest volumes and PC_{cavity} in the host frameworks of α-type and β-type structures. A wide range of the alcoholic guests (71.0–137.5 Å^3) are included in the β-type structure. In the same host framework and at the same host/guest ratio, PC_{cavity} tended to increase with an increase of the guest volume.[53,54] The plots of β-type structures with the primary alcoholic guests were linear in PC_{cavity}, indicating that the host frameworks form cavities similar in size: the cavity volumes are in the range of 507.2–550.1 Å^3. On the other hand, the plots of β-type structures with the secondary and tertiary alcoholic guests had constant PC_{cavity} values in spite of the increase of the guest volumes. This indicates that the host frameworks form flexible cavities: the cavity volumes of β-type structures with secondary and tertiary alcoholic guests were in the ranges of 588.3–775.0 and 508.8–693.0 Å^3, respectively. Such flexibility may be caused by the stacking of the helical columns mainly through van der Waals contacts. From crystallographic parameters, the β-type structure had a wide range of distances between the helical columns along their long-axis as shown in Fig. 10a. Although different distances make a wide-range inclusion behavior possible, brucine selectively cocrystallized with the guest through molecular recognition. In the next part, we describe the molecular recognition for aliphatic alcohol guests in the host cavity focusing on the β-type structure, because of the wide-range inclusion behavior.

Molecular Recognition in the Host Cavities. Crystallographic studies of brucine inclusion crystals with aliphatic alcohols indicated the following things: Tertiary amino and carbonyl groups as hydrogen-bonding acceptors in the characteristic 2_1 helical tape-like assemblies of brucine took part in hydrogen bonding with guest molecules. Moreover, primary and most secondary aliphatic alcohols tended to be connected

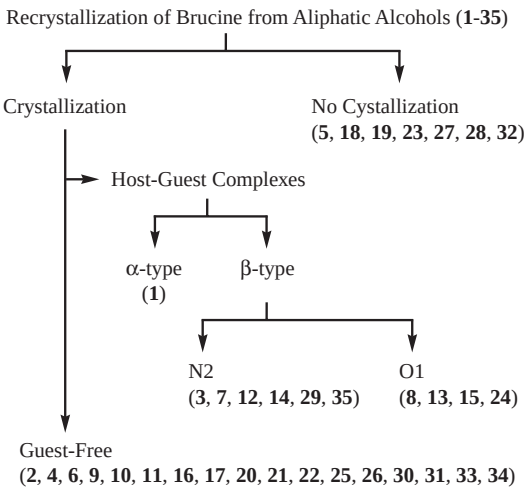

Scheme 3. Overview of crystallization studies of brucine with a series of aliphatic alcohols.

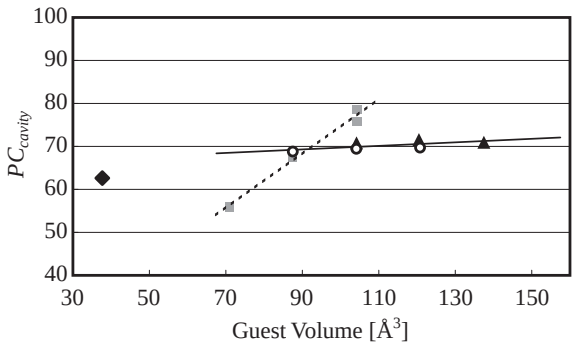

Fig. 9. The plots of PC_{cavity} of α-type (◆), β-type with primary alcohols (■), β-type with secondary alcohols (▲), and β-type with tertiary alcohols (○).

Table 3. Parameters for PC_{cavity} in Brucine Inclusion Crystals

Guest	Host/guest molar ratio	V_{guest}/Å^{3} a)	V_{cavity}/Å^{3} b)	Number of guest molecules in unit cell	PC_{cavity}/% c)
Methanol (**1**)	1:2	37.7	481.5	8	63
1-Propanol (**3**)	1:1	71.0	507.2	4	56
2-Methyl-1-propanol (**7**)	1:1	87.5	518.6	4	67
2-Methyl-2-propanol (**8**)	1:1	87.5	508.8	4	69
2-Methyl-1-butanol (**12**)	1:1	104.3	530.5	4	79
2-Methyl-2-butanol (**13**)	1:1	104.1	599.9	4	69
3-Methyl-1-butanol (**14**)	1:1	104.4	550.1	4	76
3-Methyl-2-butanol (**15**)	1:1	104.2	588.3	4	71
3-Methyl-3-pentanol (**24**)	1:1	120.8	693.0	4	70
3,3-Dimethyl-2-butanol (**29**)	1:1	120.5	673.2	4	72
2,4-Dimethyl-3-pentanol (**35**)	1:1	137.5	775.0	4	71

a) V_{guest} denotes the volume of the guest molecules calculated by HF/6-31G*. b) V_{cavity} denotes the volume of the cavity in the unit cell calculated with a 0.7 Å radius probe. c) PC_{cavity} denotes the packing coefficient of the guest molecules in the host cavity, given by the following expression: PC_{cavity} [%] = [(V_{guest}) × (number of guest molecules in unit cell)]/V_{cavity} × 100.

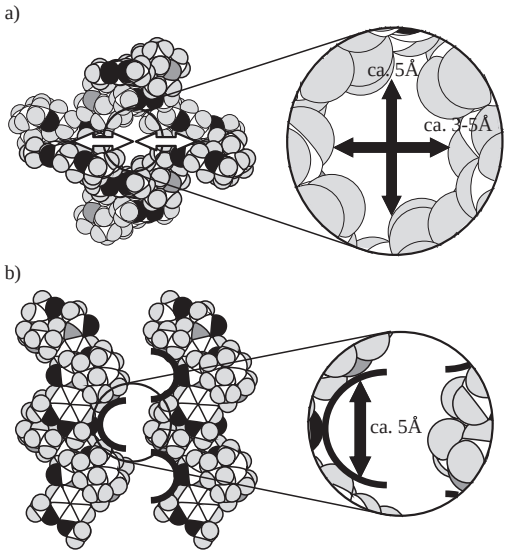

Fig. 10. Detailed views of the one-dimensional cavity in β-type structure of brucine: a) a top view, and b) a side view represented by van der Waals space-filling models. Two-headed white arrows indicate the axis along which the modulation between the helical tapes occurs easily, while four-headed black arrow does the length and width of the cavity (ca. 5, and 3–5 Å, respectively). Solid curved lines depict edges of the grooves of the helical tapes. The width of the groove is depicted by two-headed black arrow, and is ca. 5 Å. Filling the grooves with the guest substituents affords the inclusion crystals.

by a O_{guest}–H···N2 (N2: tertiary amino) hydrogen bond, while the other aliphatic alcohols were connected by a O_{guest}–H···O1 (O1: carbonyl) hydrogen bond in the brucine inclusion crystals.

Scheme 4 shows tree diagrams of the inclusion behavior of brucine and of the structural changes of host assemblies as supramolecular isomerization in connection with the increase of methylene units of the guests. We obtained the α-type structure of brucine only when guest **1** was included in a 1:2 host/guest molar ratio. However, guests **2** and **4** were not included in a 1:2 and 1:1 host/guest molar ratio in the α-type structure because of the closer and looser fits between the guest molecule and the host cavity, respectively. On the other hand, guest **3** was included with supramolecular isomerization of the host framework from α-type to β-type structures as shown in Scheme 4a. The increase of the methylene units of the guests (Schemes 4a–4c) revealed that the host framework isomerized depending on the size of the guest molecules. Moreover, it was found that the β-type structure included a wide range of aliphatic alcoholic guests (71.0–137.5 $Å^3$). Therefore, it should be possible to predict qualitatively the inclusion behavior from the size/shape fit between the guests (71.0–137.5 $Å^3$) and the host cavity in the only β-type structure below. Since the size of inclusion space of brucine is variable due to van der Waals contacts between the helical tapes, a wide range of aliphatic alcohols can be included. However, despite the versatility, brucine shows selectivity for alcoholic guests in the range C3 to C7. The guest selectivity may be related to the grooves of the helical columns as shown in Fig. 10b. The widths of the grooves are ca. 5 Å. Unless the grooves are filled with the guest substituents, inclusion crystals should not form due to the looser fit between the guest molecule and the host cavity. Besides, the length and width of host cavities, as described in Fig. 10a, must be considered when discussing the guest selectivity in relation to the guest size. From Scheme 4, the host cavity has a limit in the number of the carbon atoms between hydroxy and terminated methyl groups of the guests, which helps to explain the steric hindrance between the host cavity and the guest molecules.

As shown in Schemes 3 and 4, it is not clear experimentally whether the guests **5**, **18**, **19**, **23**, **27**, **28**, and **32** can be included. However, we may be able to predict the inclusion behavior from the systematic investigation. To predict the inclusion behavior, we need to understand the size/shape fit between the host cavity and the guest molecules and to estimate the number of the carbon atoms between hydroxy and terminated methyl groups of the guests in the inclusion crystals by the comparison of chemical structures of the guests. For example, guest **5** might be included in the β_{N2}-type structure with four carbon atoms between the hydroxy and the terminated methyl groups similar to guests **12** and **14**. Thus, the ability to form hydrogen bonds and the size/shape fit lead to a reasonable explanation.

Conclusion

We described the systematic investigation of inclusion crystals of brucine with aliphatic alcohols. These resultant crystals were elucidated by using a qualitative hierarchical structural analysis, which showed that the molecules form common 2_1 helical tape-like assemblies and that the tapes stack in different ways to give the supramolecular isomers; GF, α-type, and β-type structures (Fig. 11). We demonstrated that supramolecular isomerization of the host frameworks in brucine inclusion crystals with aliphatic alcohols occurred mainly depending on the size of the guest molecules. It is thought that three-directional chirality is a useful concept for better understanding of supramolecular isomerism. At present, using three-directional chirality, it is possible to determine the handedness of 2_1 helical tape-like assemblies of chiral compounds with similar molecular skeletons to steroidal bile acids and brucine. In order to determine the handedness of 2_1 helical assemblies in various systems, further investigations are proceeding in our laboratory.

The different types of 2_1 helical tape-like assemblies are often observed in the brucine inclusion crystals with acidic guests.[22,38,42] In this case, brucinium salts are interpreted as being single molecules due to strong charge-assisted hydrogen bonds between the host and guests. Such an interpretation can explain the acidic guest-induced supramolecular isomerism of brucine. Thus, each phase in the proposed analysis depends mainly on the strengths of intermolecular interactions. The proposed analysis will contribute to the creation of supramolecular architectures. Actually, this has recently become possible by applying the concept of hierarchical self-assembly, i.e., non-covalent organization of molecules and macromolecules that takes places over distinct multiple phases.[58] However, the design and prediction of crystal structures as high-ordered supramolecular architectures has been difficult because of appearance of unexpected supramolecular isomers.[59]

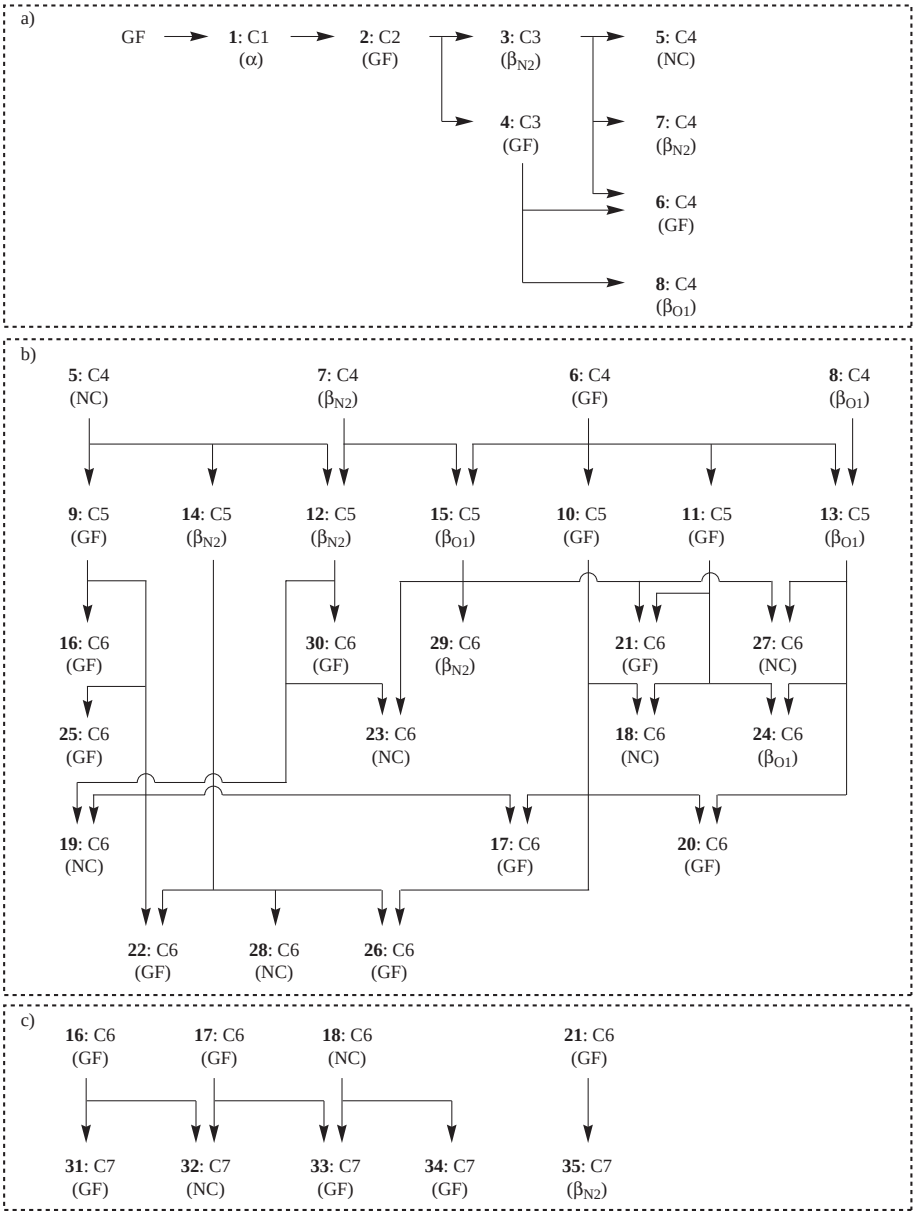

Scheme 4. Tree diagram of inclusion behavior of brucine in connection with the increase of methylene units of the guests in the range a) C0 to C4, b) C4 to C6, and c) C6 to C7, where C*n* denotes the number of the carbon atoms.

Our results show that the supramolecular isomers can be qualitatively predicted through supramolecular chirality, and promise the possibility to apply the crystal structure prediction.

In this way, qualitative hierarchical structural analysis is useful for understanding the supramolecular chirality and isomerism starting from chiral molecules, and it serves as a model for explaining complex phenomena, such as chirality evolution, nucleation, and crystallization.

Experimental

General Methods. All chemicals and solvents were commercially available and used without any purification. IR spectra were recorded on a HORIBA FT-IR spectrometer. Thermal gravimetry (TG) was performed on a Rigaku Thermoplus TG8120 with about 10 mg of sample from 30 to 300 °C at a heating rate of 5 °C min^{-1}.

Preparation of Inclusion Crystals. Brucine was dissolved by warming in the liquid guest, and the resulting solution was allowed to stand at room temperature. The resulting crystals were collected and dried on filter papers.

Crystal Structure Determinations. X-ray diffraction data were collected on a Rigaku R-AXIS RAPID diffractometer with 2D area detector with graphite-monochromated Cu Kα radiation. Lattice parameters were obtained by least-squares analysis of 25 reflections measured in the range $20^\circ \leq 2\theta \leq 25^\circ$ in the four-circle diffractometer and reflections for three oscillation images in the 2D area detector. Direct methods (SIR-92[60] and SIR-88[61]) were employed for the solution of the structures. The structures were refined by using the full-matrix least-squares procedure in the program teXsan.[62] All non-hydrogen atoms were refined with anisotropic displacement parameters, and hydrogen atoms of the host molecule were placed in idealized positions and refined as

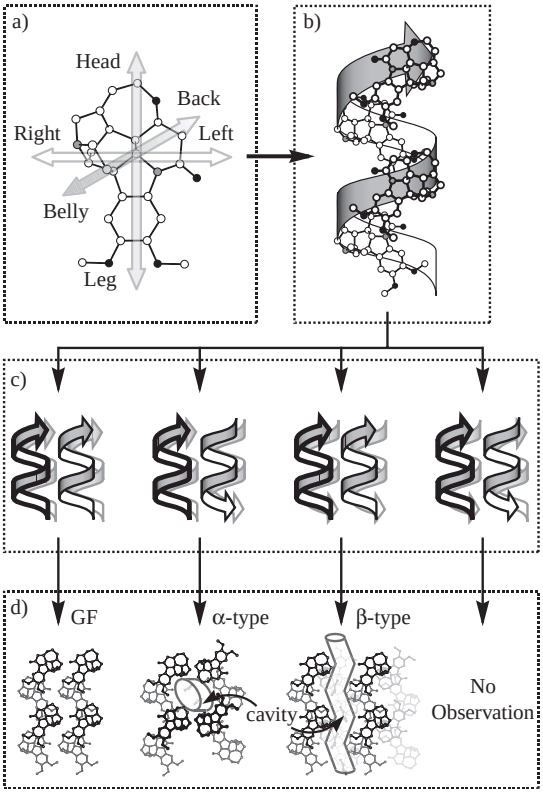

Fig. 11. Hierarchical interpretation of formation of brucine inclusion crystal structures; a) fixing a molecular conformation with three-directional chirality, b) combining the bimolecular aggregate to form a helical tape-like assembly with supramolecular chirality, c) stacking the tapes in a parallel or anti-parallel fashion to produce a bundle, and d) accommodating guest molecules in the cavities of the bundles.

rigid atoms with the relative isotropic displacement parameters.

The hydrogen atoms of the guest molecules were placed in idealized positions, and no further refinement was applied. The assignments of **3**, **12**, **14**, and **15** in the inclusion crystals were not determined because of disorder. All calculations were performed using the teXsan crystallographic software package.

Crystallographic data have been deposited with Cambridge Crystallographic Data Centre: Deposition numbers CCDC-626955–626965 for compounds brucine·**1**, **3**, **7**, **8**, **12**, **13**, **14**, **15**, **24**, **29**, and **35**. Copies of the data can be obtained free of charge via http://www.ccdc.cam.ac.uk/conts/retrieving.html (or from the Cambridge Crystallographic Data Centre, 12, Union Road, Cambridge, CB2 1EZ, UK; Fax: +44 1223 336033; e-mail: deposit@ccdc.cam.ac.uk).

Calculations. The volumes of the guest molecules were obtained by HF calculations at the level of 6-31G* using Spartan'04.[63] The volumes of the host cavities were derived from the atomic coordinates by using the Free Volume program,[64] in the Cerius2 software package.[65] The atomic radii [Å] used here are as follows: 1.20 for hydrogen, 1.70 for carbon, 1.65 for nitrogen, 1.60 for oxygen.

T. Watabe expresses his special thanks for the center of excellence (21COE) program "Creation of Integrated EcoChemistry of Osaka University." This work was supported by a Grant-in-Aid for Scientific Research on Priority Areas (No. 17034039) from the Ministry of Education, Culture, Sports, Science and Technology, Japan.

Supporting Information

Figures S1–S4 show TG spectra of the brucine inclusion crystals with **3**, **12**, **14**, and **15** in PDF format. Figures S5–S9 show IR spectra of the guest-free and inclusion crystals with **3**, **12**, **14**, and **15** in PDF format. These materials are available free of charge on the web at http://www.csj.jp/journals/bcsj/.

References

1 Reviews: a) *Inclusion Compounds*, ed. by J. L. Atwood, J. E. D. Davies, D. D. Macnicol, Academic Press, London, **1984**, Vols. 1–3; *Inclusion Compounds*, ed. by J. L. Atwood, J. E. D. Davies, D. D. MacNicol, Oxford Press, Oxford, **1991**, Vols. 4 and 5. b) *Top. Curr. Chem.* ed. by E. Weber, Springer-Verlag, London, U.K., **1987**, Vol. 140; **1988**, Vol. 149. c) *Comprehensive Supramolecular Chemistry, Solid-State Supramolecular Chemistry: Crystal Engineering*, ed. by D. D. MacNicol, F. Toda, R. Bishop, Pergamon, Oxford, **1996**, Vol. 6. d) *Nanoporous Materials: Science and Engineering*, ed. by G. Q. Lu, X. S. Zhao, Imperial College Press, London, **2004**.

2 A. M. Pivovar, K. T. Holman, M. D. Ward, *Chem. Mater.* **2001**, *13*, 3018.

3 G. R. Desiraju, *Nature* **2001**, *412*, 397.

4 M. D. Hollingsworth, *Science* **2002**, *295*, 2410.

5 J. L. Atwood, L. J. Barbour, A. Jerga, *Science* **2002**, *296*, 2367.

6 K. T. Holman, A. M. Pivovar, J. A. Swift, M. D. Ward, *Acc. Chem. Res.* **2001**, *34*, 107.

7 K. T. Holman, S. M. Martin, D. P. Parker, M. D. Ward, *J. Am. Chem. Soc.* **2001**, *123*, 4421.

8 K. Kobayashi, A. Sato, S. Sakamoto, K. Yamaguchi, *J. Am. Chem. Soc.* **2003**, *125*, 3035.

9 S. Aitipamula, A. Nangia, *Chem. Eur. J.* **2005**, *11*, 6727.

10 M. Miyata, K. Sada, in *Comprehensive Supramolecular Chemistry, Solid-State Supramolecular Chemistry: Crystal Engineering*, ed. by D. D. MacNicol, F. Toda, R. Bishop, Pergamon, Oxford, **1996**, Vol. 6, p. 147.

11 M. Miyata, K. Sada, N. Yoswathananont, in *Encyclopedia of Supramolecular Chemistry*, ed. by J. L. Atwood, J. W. Steed, Marcel Dekker, New York, **2004**, Vol. 1, p. 441.

12 K. Kato, M. Sugahara, N. Tohnai, K. Sada, M. Miyata, *Cryst. Growth Des.* **2004**, *4*, 263.

13 K. Kato, K. Inoue, N. Tohnai, M. Miyata, *J. Inclusion Phenom. Macrocyclic Chem.* **2004**, *48*, 61.

14 K. Kato, M. Sugahara, N. Tohnai, K. Sada, M. Miyata, *Eur. J. Org. Chem.* **2004**, 981.

15 K. Kato, N. Tohnai, M. Miyata, *Mol. Cryst. Liq. Cryst.* **2005**, *440*, 125.

16 T. Watabe, K. Kato, N. Tohnai, M. Miyata, in *Structure and Dynamics in Macromolecular Systems with Specific Interactions*, ed. by K. Adachi, T. Sato, Osaka University Press, **2005**, Vol. 1, p. 157.

17 T. Watabe, K. Kobayashi, K. Kato, K. Sada, M. Miyata, *Mol. Cryst. Liq. Cryst.* **2005**, *440*, 117.

18 T. Watabe, D. Yoshikawa, I. Hisaki, N. Tohnai, M. Miyata, *Chem. Lett.* **2006**, *35*, 806.

19 R. O. Gould, M. D. Walkinshaw, *J. Am. Chem. Soc.* **1984**, *106*, 7840.

20 G. Quinkert, H.-G. Schmalz, E. M. Dzierzynski, G. Durner, J. W. Bats, *Angew. Chem., Int. Ed. Engl.* **1986**, *25*, 992.
21 S. E. Boiadjiev, R. V. Person, C. Puzicha, C. Knobler, E. Maverick, K. N. Trueblood, D. A. Lightner, *J. Am. Chem. Soc.* **1992**, *114*, 10123.
22 S. Kuwata, J. Tanaka, N. Onda, T. Yamada, T. Miyazawa, M. Sugiura, Y. In, M. Doi, M. Inoue, T. Ishida, *Bull. Chem. Soc. Jpn.* **1993**, *66*, 1501.
23 J. L. Wright, B. W. Caprathe, D. M. Downing, S. A. Glase, T. G. Heffner, J. C. Jaen, S. J. Johnson, S. R. Kesten, R. G. MacKenzie, L. T. Meltzer, T. A. Pugsley, S. J. Smith, L. D. Wise, D. J. Wustrow, *J. Med. Chem.* **1994**, *37*, 3523.
24 F. J. J. Dijksma, R. O. Gould, S. Parsons, P. Taylor, M. D. Walkinshaw, *Chem. Commun.* **1998**, 745.
25 K. Krajewski, Z. Ciunik, *Pol. J. Chem.* **1999**, *73*, 1687.
26 J. B. Laursen, C. G. Jorgensen, J. Nielsen, *Bioorg. Med. Chem.* **2003**, *11*, 723.
27 A. Białońska, Z. Cinuik, *CrystEngComm* **2004**, *6*, 276.
28 A. Białońska, Z. Cinuik, T. Popek, T. Lis, *Acta Crystallogr., Sect. C* **2005**, *61*, o88.
29 A. Białońska, Z. Cinuik, *CrystEngComm* **2006**, *8*, 66.
30 A. Białońska, Z. Cinuik, *Acta Crystallogr., Sect. C* **2004**, *60*, o853.
31 S. S. B. Glover, R. O. Gould, M. D. Walkinshaw, *Acta Crystallogr., Sect. C* **1985**, *41*, 990.
32 A. A. Pinkerton, P.-A. Carrupt, F. Claret, P. Vogel, *Acta Crystallogr., Sect. C* **1993**, *49*, 1632.
33 K. Chandramohan, K. Ravikumar, *J. Chem. Crystallogr.* **1999**, *29*, 121.
34 G. Smith, U. D. Wermuth, P. C. Healy, J. M. White, *Acta Crystallogr., Sect. C* **2006**, *62*, o203.
35 F. Toda, K. Tanaka, H. Ueda, *Tetrahedron Lett.* **1981**, *22*, 4669.
36 M. Yamagishi, Y. Yamada, K. Ozaki, T. Da-te, K. Okamura, M. Suzuki, K. Matsumoto, *J. Org. Chem.* **1992**, *57*, 1568.
37 J. Bao, W. D. Wulff, J. B. Dominy, M. J. Fumo, E. B. Grant, A. C. Rob, M. C. Whitcomb, S.-M. Yeung, R. L. Ostrander, A. L. Rheingold, *J. Am. Chem. Soc.* **1996**, *118*, 3392.
38 F. J. J. Dijksma, R. O. Gould, S. Parsons, M. D. Walkinshaw, *Acta Crystallogr., Sect. C* **1998**, *54*, 1948.
39 K. Sada, K. Yoshikawa, M. Miyata, *Chem. Commun.* **1998**, 1763.
40 E. Cheung, M. R. Netherton, J. R. Scheffer, J. Trotter, *Tetrahedron Lett.* **1999**, 8737.
41 S. Allenmark, U. Skogsberg, *Enantiomer* **2000**, *5*, 451.
42 G. Smith, U. D. Wermuth, D. J. Young, P. C. Healy, *Acta Crystallogr., Sect. E* **2005**, *61*, o2008.
43 G. Smith, U. D. Wermuth, P. C. Healy, D. J. Young, J. M. White, *Acta Crystallogr., Sect. E* **2005**, *61*, o2646.
44 A. Białońska, Z. Cinuik, *Acta Crystallogr., Sect. E* **2005**, *61*, o4222.
45 A. Białońska, Z. Cinuik, *Acta Crystallogr., Sect. C* **2006**, *62*, o182.
46 J. P. M. Lommerse, W. D. S. Motherwell, H. L. Ammon, J. D. Dunitz, A. Gavezzotti, D. W. M. Hofmann, F. J. J. Leusen, W. T. M. Mooij, S. L. Price, B. Schweizer, M. U. Schmidt, B. P. van Eijck, P. Verwer, D. E. Williams, *Acta Crystallogr., Sect. B* **2000**, *56*, 697.
47 W. D. S. Motherwell, H. L. Ammon, J. D. Dunitz, A. Dzyabchenko, P. Erk, A. Gavezzotti, D. W. M. Hofmann, F. J. J. Leusen, J. P. M. Lommerse, W. T. M. Mooij, S. L. Price, H. Scheraga, B. Schweizer, M. U. Schmidt, B. P. van Eijck, P. Verwer, D. E. Williams, *Acta Crystallogr., Sect. B* **2002**, *58*, 647.
48 A. Gavezzotti, *CrystEngComm* **2002**, *4*, 343.
49 G. M. Day, W. D. S. Motherwell, H. L. Ammon, S. X. M. Boerrigter, R. G. Della Valle, E. Venuti, A. Dzyabchenko, J. D. Dunitz, B. Schweizer, B. P. van Eijck, P. Erk, J. C. Facelli, V. E. Bazterra, M. B. Ferraro, D. W. M. Hofmann, F. J. J. Leusen, C. Liang, C. C. Pantelides, P. G. Karamertzanis, S. L. Price, T. C. Lewis, H. Nowell, A. Torrisi, H. A. Scheraga, Y. A. Arnautova, M. U. Schmidt, P. Verwer, *Acta Crystallogr., Sect. B* **2005**, *61*, 511.
50 A. I. Kitaigorodskii, *Molecular Crystals and Molecules*, Academic Press, London, **1973**.
51 T. Hahn, *International Tables for Crystallography, Vol. A: Space-Group Symmetry*, Kluwer Academic Publishers, London, **1983**.
52 I. Hisaki, T. Watabe, Y. Kogami, N. Tohnai, M. Miyata, *Chem. Lett.* **2006**, *35*, 1274.
53 K. Nakano, K. Sada, Y. Kurozumi, M. Miyata, *Chem. Eur. J.* **2001**, *7*, 209.
54 N. Yoswathananont, K. Sada, K. Nakano, K. Aburaya, M. Shigesato, Y. Hishikawa, K. Tani, N. Tohnai, M. Miyata, *Eur. J. Org. Chem.* **2005**, 5330.
55 S. Mecozzi, J. Rebek, Jr., *Chem. Eur. J.* **1998**, *4*, 1016.
56 G. R. Desiraju, *Crystal Engineering: The Design of Organic Solids*, Elsevier, New York, **1989**.
57 A. Gavezzotti, *Acc. Chem. Res.* **1994**, *27*, 309.
58 J. A. A. W. Elemans, A. E. Rowan, R. J. M. Nolte, *J. Mater. Chem.* **2003**, *13*, 2661.
59 V. R. Vangala, R. Mondal, C. K. Broder, J. A. K. Howard, G. R. Desiraju, *Cryst. Growth Des.* **2005**, *5*, 99.
60 A. Altomare, G. Cascarano, C. Giacovazzo, A. Guagliardi, M. C. Burla, G. Polidori, M. Camalli, *J. Appl. Crystallogr.* **1994**, *27*, 435.
61 M. C. Burla, M. Camalli, G. Cascarano, C. Giacovazzo, G. Polidori, R. Spagna, D. Viterbo, *J. Appl. Crystallogr.* **1989**, *22*, 389.
62 *teXsan, Crystal Structure Analysis Package*, Molecular Structure Corporation.
63 *Spartan'04, Molecular Modeling Software*, Wavefunction Inc.
64 R. Voorintholt, M. T. Kosters, G. Vegter, G. Vriend, W. G. J. Hol, *J. Mol. Graphics* **1989**, *7*, 243.
65 *Cerius*^{2}, *Molecular Simulation Software*, Molecular Simulation Inc.